

In-Situ Manipulation of Superconducting Properties via Ultrasonic Excitation

Biswajit Dutta¹ and A. Banerjee²

¹*Ecole Normale Supérieure de Lyon, CNRS, Laboratoire de Physique, F-69342 Lyon, France*

²*UGC-DAE Consortium for Scientific Research, University Campus, Khandwa Road, Indore-452001, India.*

We demonstrate in-situ manipulation of the critical temperature (T_S) and upper critical field (H_{C2}) of conventional and unconventional superconductors via ultrasonic excitation. Utilizing DC magnetization and AC susceptibility measurements, we observed a reduction in both T_S and H_{C2} with increasing amplitude of the applied ultrasonic waves. This reduction exhibits a power law dependence on the excitation voltage, suggesting a non-linear coupling between the ultrasonic waves and the superconducting order parameter. Measurements on a paramagnetic material (Gd_2O_3) with quenched orbital angular momentum ($L=0$) revealed no change in magnetization even under extreme ultrasonic excitation amplitude, highlighting the role of spin-orbit coupling in the observed effects. Similar measurements on cuprate superconductors showed analogous behavior, suggesting a possible link between the observed modification of superconducting properties and the modulation of the antiferromagnetic network by ultrasonic excitation.

PACS numbers: 75.47.Lx, 71.27.+a, 75.40.Cx, 75.60.-d

I. INTRODUCTION

The magnetization (M), electric polarization (P) and strain tensor (ϵ) are three fundamental important order parameters in condensed matter physics. The external parameters like magnetic field (H), electric field (E) and the force tensor (σ) to control M, P and ϵ , respectively. In the multiferroic material the cross correlation between M and P is observed i.e. M can be controlled by H and E both, along with that P can also be controlled by E and H. Therefore because of this cross correlation the functionality of the material increases for device application. Similarly both M and P can be controlled by σ in high pressure experiment, because the electronic functionality originates from the crystal structure with translational symmetry and application of external pressure disturbs the translational symmetry by disturbing the lattice. The hydrostatic expansion is expected to decrease the electron hopping and there by increase the electron lattice coupling, which resulting in a lower value of Curie temperature (T_C), where as the hydrostatic compression shows the opposite behavior of expansion [1]. So these observations suggest that change of T_C depends on the type of structural change, i.e. hydrostatic compression or anisotropic compression accompanied by tensile and compressive strain [1]. Y. Moritomo et al., [2] has reported in $\text{La}_{(1-x)}\text{Sr}_x\text{MnO}_3$ ($0.15 \leq x \leq 0.5$) pressure stabilizes the ferromagnetic metallic state by enhancing the transfer interaction. $\text{La}_{0.7}\text{Sr}_{0.3}\text{MnO}_3$ is observed to destabilize the ferromagnetic metallic state along with decrement of T_C (~ 10 K) while increasing the tensile strain [3]. The superconducting transition temperature (T_S) is also observed to increase with increasing the hydrostatic pressure in lanthanum based hole doped cuprate superconductor where as in case of electron doped Lanthanum based superconductor T_S does not vary with hydrostatic pressure [4]. In case of a thin film the stretching (squashing) of CuO_6 octahedra enhances (decreases) T_S [5–8], but this type of modulation is static and irreversible in

nature hence difficult for technological application, because the deformation has to be reversible and dynamical as well for any kind of technological application. The possible solution for this is the ultrasonic shock wave. In this case the applied stress is function of time and results in a diffusive acoustic strain. Due to spin-orbit interaction and dipolar field the spins experience elastic deformation when the lattice is excited by an elastic wave, this type of coupling is known as magnetoelastic coupling (MEC) and the opposite effect is known as magnetostriction (i.e. the lattice is deformed due to the change of magnetization) [9–11]. Therefore if the frequency and wave length of spin wave in a crystal lattice become comparable to the the frequency and wave length of the elastic wave then probability of MEC increases or hybridization of spin-lattice excitation (i.e magnon-phonon hybridization) is observed, this coupling phenomena between elastic and magnetic dynamic was first theoretically investigated almost six decades ago by C.Kittel [12]. This field has been attracted much more attention in recent times because of improved material growth technique and device fabrication methods [13–16].

Recently in transverse spin Seebeck effect measurement acoustic wave has been used to pump spins in ferromagnet and MEC is concluded as the possible mechanism for the appearance of this effect [13, 14]. Ferromagnetic resonance of Cobalt film is also observed to get enhanced by pulsed surface acoustic wave [16]. The manipulation of Meissner effect of cuprate superconductor $\text{YBa}_2\text{Cu}_3\text{O}_7$ (YBCO) [19] and $\text{Bi}_2\text{Sr}_2\text{Ca}_2\text{Cu}_3\text{O}_{10}$ (BSCCO(2223)) [20] is observed by dynamical acoustic strain, which indicates the importance of phonon contribution on the electron pairing mechanism of cuprate superconductor. The contribution of phonon to the superconductivity of cuprate superconductor is still under debate, the oxygen isotope (O^{18}) effect measurement depicts the phonon contribution to the electron pairing mechanism is not simply follows the BCS theory [21–26]. The wavelength of the present acoustic wave is of the order of millimeter range,

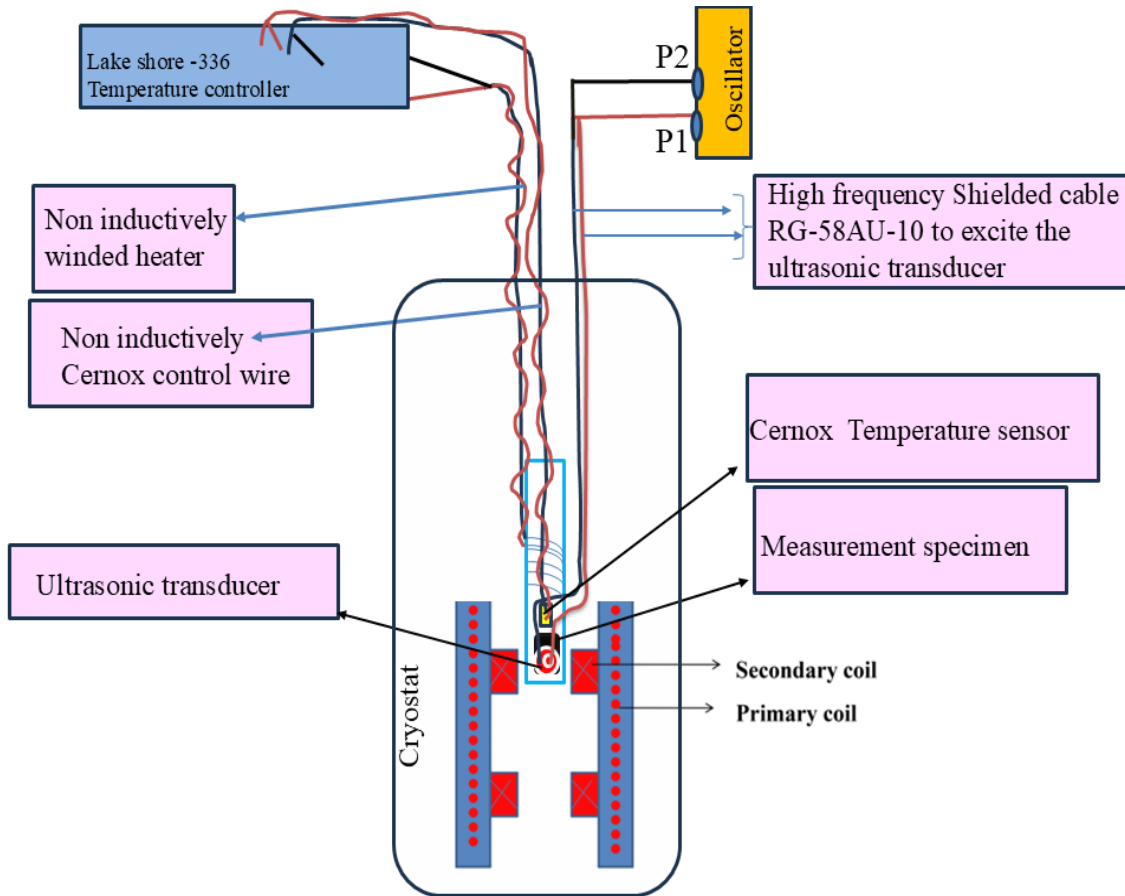


FIG. 1. (Colour Online) The experimental arrangement for ultrasonic excitation during magnetization measurement.

hence resulting in the long-ranged spatial modulation of the lattice and considering the energy scale the effect is considered as the modulation of acoustic phonons, therefore any property coupled with these acoustic phonon is definitely affected by the ultrasonic wave.

A. Experimental set-up

The assembly of the experimental setup is shown in FIG. 1. We have performed this measurement in a home built ac susceptibility set up[27]. It shows the concentric assembly of the primary and the secondary coil, a Lock-In amplifier (Sanford Research Systems model SR830) is used to excite the primary coil by the ac field, as well as for the measurement of the induced response from the secondary coils in differential mode. The temperature controlling and measurements are done by a temperature controller LakeShore model-336 and using Cernox sensor, respectively. The sample holder is made of single crystal sapphire rectangular bar of length 7 cm and width 0.5 cm and thickness of 0.2 cm, this sapphire rectangular bar is grooved with a SS rod via a 10cm long hylum rod for better thermal isolation. A non inductively wounded heater

wire (to minimize magnetic contribution from the heater current) and the Cernox temperature sensor is placed on the same sapphire bar. The 10MHz ultrasonic transducer made of LiNbO₃ is attached on the sample by very thin layer of stopcock grease and the transducer is excited from out side by using a high frequency function generator and high frequency cable (RG-58AU-10 of outer diameter 2.9 mm) is soldered in the transducer for the electrical connection. Measurements are performed in the following protocols, initially the system is cooled to a desire temperature, then transducer is excited by an desirable 10 MHz sinusoidal voltage and in this condition the temperature dependent ac susceptibility measurements are performed. Then after the final scan the transducer voltage is turned off and again the system has been cooled to the desirable temperature and theses process are repeated for all measurements. Similar procedures are followed for the magnetic isotherm measurement in SQUID magnetometer, in this case we have attached some wires (RG-58AU-10 of outer diameter 2.9 mm) with the sample holder of SQUID magnetometer to apply the sinusoidal voltage (out side from the SQUID magnetometer cryostat) to the transducer glued on the sample by stopcock grease.

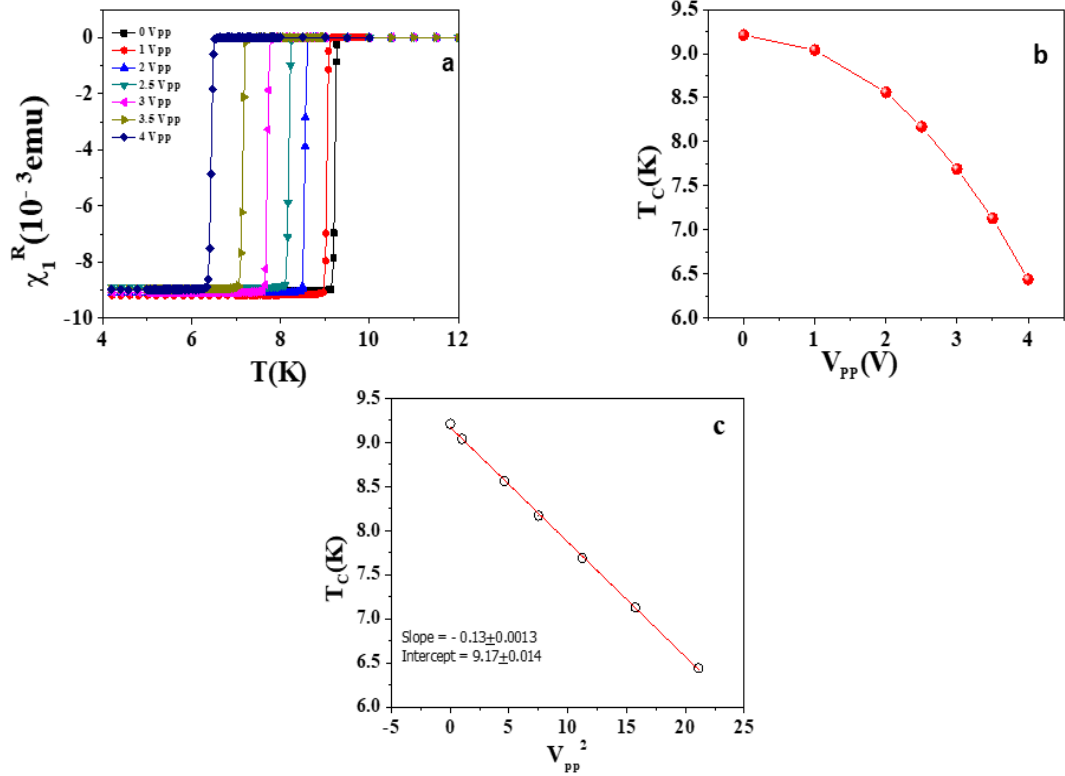


FIG. 2. (Colour Online) The measurements are performed on Nb, A "Y" cut, 10 MHz LiNbO₃ crystal is used to excite the superconductor. The susceptibility measurements are performed in an ac field of amplitude 1 Oe and frequency 231.1 Hz (a) The real part of first order susceptibility (χ_1^R) is plotted against temperature and the corresponding V_{PP} is 0, 1, 2, 2.5, 3, 3.5, 4 V respectively. (b) T_C (K) is plotted against V_{PP} . (c) linearized plot of T_C (K) against V_{PP}^2 .

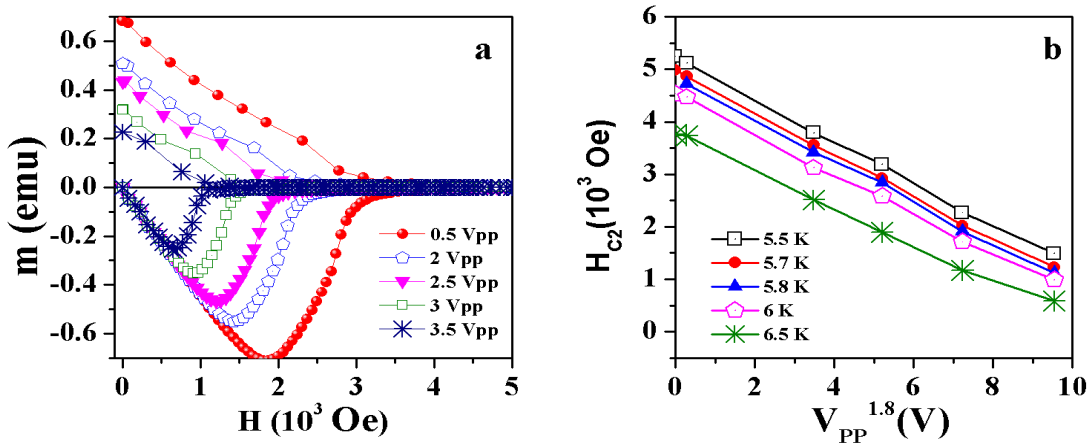


FIG. 3. (Colour Online) The measurements are performed on Nb, A "Y" cut, 10 MHz LiNbO₃ crystal is used to excite the superconductor. (a) Magnetic isotherms at 5 K and the corresponding excitation voltage V_{PP} is 0.5, 2, 2.5, 3, 3.5 V respectively. (b) H_{C2} (K) is plotted against $V_{PP}^{1.8}$ at 5.5 K, 5.7 K, 5.8 K, 6 K, 6.5 K.

B. Study on Niobium (Nb)

Niobium (Nb) is a transition metal and shows conventional superconductivity below 9.25 K (superconducting transition temperature (T_C)) [28] i.e. electron pairing

is mediated by electron-phonon coupling (Follows BCS theory). Nb is mostly used in superconducting radio frequency cavity application [29]. The hydrostatic pressure dependent study on Nb depicted a decrement of superconducting transition temperature with the increment of hydrostatic pressure and change in temperature with the

application of hydrostatic pressure follows the relation corresponding to -0.02 K/GPa [30]. The superconducting property of Nb is also observed to be controlled by using epitaxial strain [31–33]. However these above approaches for the manipulation of phase transition and physical property of the superconductor are stationary or independent of time, hence these methods are not favorable for high speed manipulation in device application.

Here we have manipulated the phase transition by applying dynamical acoustic strain. Generally acoustic waves have been used to evaluate the elastic constant and sound velocity in any material, along with that the magnetic response of that system also modifies via MEC or spin-orbit coupling, electron-phonon coupling etc. However, we have used the piezoelectric transducer (LiNbO_3) as the source of time-dependent stress which acts as an external perturbation on the physical state of the superconductor. The temperature dependent ac susceptibility graph of Nb at different dynamical excitation amplitude (i.e. V_{PP} of frequency 10 MHz) is shown in FIG. 2a, it shows the onset temperature of diamagnetism decreases to lower temperature when the amplitude of dynamical stress increases, here it is also observed that the transition remain sharper against temperature at maximum values of ultrasonic voltage, which indicates the excitation distributed uniformly throughout the bulk of Nb, other wise distribution of stress amplitude could have cause broadening in the superconducting transition temperature. At $4V_{PP}$ the T_C is observed around 6.25 K , exhibits reduction almost about 3 K . The variation of T_C against V_{PP} is shown in FIG. 2b, it shows T_C decreases by following the square of V_{PP} i.e. the mathematical relation between T_C and V_{PP} is as follows,

$$T_C = 9.22 * [1 - (\frac{V_{PP}}{7.31})^2] \quad (1)$$

It describes the magnitude of ultrasonic strain on Nb is proportional to the power consumed by the transducer. It also depicts that at $V_{PP}=7.31\text{ V}$, T_C of Nb will become zero or electron pairing will not possible at this condition. The scaled voltage dependent curve of T_C is shown in FIG. 2c, which depicts a proper straight line graph with a negative slope, this observation also verifies the square law behavior of T_C against V_{PP} .

The magnetic isotherm of Nb at 5 K and at different superimposed voltages are shown in FIG. 3a. It shows the hysteresis loop area reduces with increasing the amplitude of V_{PP} along with that H_{C2} and H_{C1} is also observed to shift to lower temperature with increasing the amplitude of V_{PP} . The behavior of H_{C2} against V_{PP} at different temperature (i.e. 5.5 K , 5.7 K , 5.8 K , 6 K , 6.5 K) is shown in FIG. 3b, it shows a power law dependent behavior (i.e. $(V_{PP})^{1.8}$ at all temperature, the value of the power is found almost close to 2). Hence both H_{C2} and T_C changes due to the dynamical excitation and follows a square law behavior. So the thermodynamical critical parameters of a conventional superconductor can be manipulated by applying dynamical stress and these

changes are found reversible also. So the ultrasonic excitation can be used in dynamic switch circuitry for ultra fast manipulation of superconductivity.

C. Study on $\text{YBa}_2\text{Cu}_3\text{O}_7$ (YBCO)

$\text{YBa}_2\text{Cu}_3\text{O}_7$ (YBCO) is a high T_C cuprate superconductor and the electron pairing mechanism of this superconductor can not be explained by using conventional BCS theory or low energy phonon mediated electron pairing. Fig. 4a shows the in phase ac susceptibility plot of YBCO at different amplitude of dynamical strain (i.e. V_{PP}). The sharp decrement of the diamagnetic fraction at $V_{PP}=0\text{ V}$ depicts good quality of the superconductor (i.e. the oxygen stoichiometry of every individual grain is almost same), along with that the similar sharpness of the decrement of diamagnetic fraction at maximum V_{PP} indicates the equal distribution of the excitation over the whole volume of the pallet, it shows T_C shifts to lower temperature with increase in the amplitude of V_{PP} . The dependence of T_C on V_{PP} is shown in Fig. 4b. T_C decreases proportionally to the square of V_{PP} and the corresponding relation is given in Eqn. 6.2

$$T_C = 91.44 * [1 - (\frac{V_{PP}}{37.78})^2] \quad (2)$$

The equation looks similar as Eqn. 6.1, the only difference is the value of the voltage (i.e. $V_{PP}=37.78\text{ V}$) at which T_C will reach to zero or YBCO will go to the normal state.

D. Study on Gd_2O_3 ($L=0$)

The real part of susceptibility (i.e. χ_1^R) of Gd_2O_3 (GdO) at zero values of dynamic excitation amplitude (i.e. $V_{PP}=0\text{ V}$) is shown in Fig. 5 along with that the susceptibility graph at $V_{PP}=10\text{ V}$ is also plotted. There is no change of the susceptibility value of GdO is observed at the maximum value of V_{PP} also, obtained from the subtracted susceptibility plot (i.e. $[\chi_1^R]_{10V_{PP}} - [\chi_1^R]_{0V_{PP}}$). Which indicates that no change in magnetic susceptibility value even at maximum applied voltage (We have also performed the measurements at intermediate voltages, results are not shown for clarity), which indicates the Curie Weiss temperature (θ_C) and effective magnetic moment (μ_{eff}) remains same after exciting the system by ultrasonic excitation. The reason behind this is zero value of spin-Orbit (or spin-lattice) coupling. According to Russell–Saunders coupling scheme the ground state of Gd^{+3} ions can be represented as $8S_{\frac{7}{2}}$, depicting that Gd^{+3} ion is isotropic in nature (or $L=0$), therefore spin-orbit coupling is absent in GdO and spins only contribute to the magnetic property of GdO [34, 35]. Hence the result of GdO depicts the material having zero values of spin-orbit (or L-S) coupling is only going to show changes

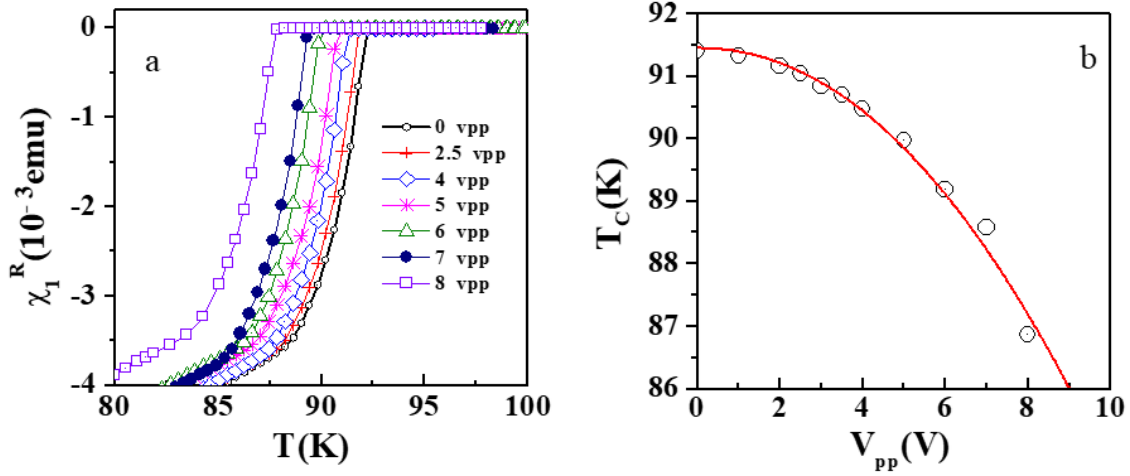


FIG. 4. (Colour Online) The measurements are performed on YBCO, A "Y" cut, 10 MHz LiNbO_3 crystal is used to excite the superconductor. The susceptibility measurements are performed in an ac field of amplitude 1 Oe and frequency 231.1 Hz (a) The real part of first harmonic (χ_1^R) is plotted against temperature and the corresponding V_{PP} is 0, 2.5, 4, 5, 6, 7, 8 V respectively. (b) T_C (K) is plotted against V_{PP} .

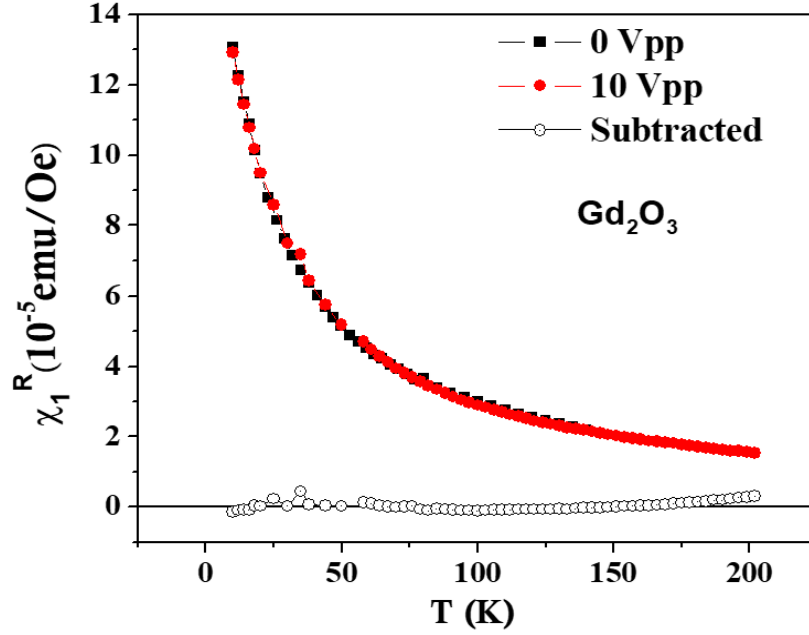


FIG. 5. (Colour Online) The measurements are performed on Gd_2O_3 , A "Y" cut, 10 MHz LiNbO_3 crystal is used to excite the paramagnet. The susceptibility measurements are performed in an ac field of amplitude 1 Oe and frequency 231.1 Hz. The real part of first order ac susceptibility (χ_1^R) is plotted against temperature and the perturbing ultrasonic voltage is $V_{PP} = 0$ V and 10 V.

in the magnetic property while the system is excited by the ultrasonic excitation. As GdO has zero values of L-S coupling, due to this reason there is no change of the magnetic property is observed when GdO is excited by an ultrasonic excitation or acoustic wave.

E. Discussion

Nb is a conventional superconductor, hence the cooper pairing is mediated by low energy phonon, due to this reason while the system is excited by the ultrasonic wave then electron scattering enhances due to the modulation

of phonon frequency and hence the probability of electron phonon coupling reduces. Due to this reason the $T_{S(onsset)}$ shifts towards lower temperature with increasing the amplitude of ultrasonic voltage.

In case of YBCO, T_C is also observed to decrease with increasing the amplitude of ultrasonic voltage in the similar manner as observed in case of Nb, indicates the involvement of low energy phonon in the electron pairing mechanism of cuprate superconductor, which is quite debated till today [21–26]. In case of Nb, $4 V_{PP}$ sinusoidal voltage is required to reduce the T_C about 3 K, where as in case YBCO almost $7 V_{PP}$ sinusoidal voltage is required to reduce the temperature about 3 K, which indicates the coefficient (also the nature) of electron phonon coupling in both the superconductors are different. These difference can be compared with the isotope effect in superconductor. According to BCS theory the shift in superconducting transition temperature (T_C) with isotope mass (M) decides the electron phonon coupling coefficient of any superconductor [21, 22],

$$\frac{\delta T_C}{T_C} = \alpha \frac{\delta M}{M} \quad (3)$$

Where α is partial isotope shift factor [21]. In the weak coupling limit T_C is given by

$$T_C = 1.13\theta_D \exp\left(-\frac{1}{\lambda}\right) \quad (4)$$

λ is electron phonon coupling constant and weakly depends on M , where as θ_D is Debye temperature and proportional to $M^{-0.5}$. The different isotope mass simply changes the Debye frequency, which affects the value of T_C [21]. In case of conventional superconductor the value of α is observed around 0.5, whereas in case of cuprate superconductor this number is observed to vary from 0.03 to 0.16 [22]. There are several controversies in the existing literature regarding the involvement of phonon in the cooper pairing mechanism of high temperature cuprate superconductor [22–26]. The angle resolved photo emission spectroscopy (ARPES) measurement depicted, the O^{18} isotope doping affect the system in a particular energy window which lies in the range of 100-300 meV [24] and these energy window is observed to coincide with the energy range of J and $2J$, where J is the super-exchange interaction of neighboring copper spins [24, 25] (i.e. the modulation of Debye frequency also modulates the AFM network in cuprate superconductors). The ultrasonic wave is an acoustic wave and its wavelength is of the millimeter order, hence resulting in the long-ranged spatial modulation of the lattice and this modulation can also affect the antiferromagnetic network in the CuO_2 plane by

spin-lattice (or spin-orbit) coupling. So the reduction of T_C due to ultrasonic excitation indicates the modulation of antiferromagnetic network (J) of the CuO_2 plane. Our previous experiments on ferromagnet and superconductor composite has also depicted the similar conclusion, in that work we have observed that the superconductivity of the cuprate superconductor is effected when the AFM interaction between the Cu^{+2} spins are modulated due to the exchange field of the ferromagnet [37]. So, further studies are required on ultrasonic excitation induced change of the magnetic property of superconductor having different hole concentration, because the AFM correlation length of cuprate superconductor is different in different hole doped region. Hence, this type of study can also provide a path way to find out the correlation between AFM fluctuation and superconductivity in the cuprate superconductor.

F. Conclusion

This study demonstrates a novel method for manipulating both orbital and lattice excitations (phonons) in materials. This is achieved through the application of ultrasonic excitation, which allows for in-situ control of these degrees of freedom. The effectiveness of this technique was confirmed by observing the influence of ultrasonic excitation on the magnetic properties of a paramagnetic salt, Gd_2O_3 . This material was chosen due to its lack of orbital angular momentum ($L=0$), ensuring that any observed changes are solely attributable to phonon modulation. The absence of local heating effects due to ultrasonic excitation was confirmed by the unchanged magnetic susceptibility at high excitation levels.

Furthermore, we demonstrated the ability to manipulate the energy gap of a conventional superconductor (Nb) using ultrasonic excitation. This finding holds potential for applications in various superconducting quantum devices. This work also opens new avenues for investigating the role of phonons in high- T_C cuprate superconductors. Specifically, it suggests that the observed decrease in the superconducting transition temperature of cuprates under ultrasonic excitation may be linked to the manipulation of the antiferromagnetic network by phonons.

G. Acknowledgment

This paper is dedicated to the memory of the late Dr. Alok Banerjee. The authors would also like to acknowledge Dr. Santanu De for his help with measurements and Er. Kranti Kumar Sharma for insightful discussions.

[1] A. J. Millis et al., J. Appl. Phys. **83**, 1588 (1998).

[2] Y. Moritomo et al., Phys. Rev. B **51**, 16491 (1995).

- [3] J. Heidler et al., Phys. Rev. B **91**, 024406(2015).
- [4] S. Arumugam et al., International Journal of Modern Physics B, **14**, 3328 (2000).
- [5] I. Bozovic et al., Phys. Rev. Lett. **89**, 107001 (2002).
- [6] J. P. Locquet et al., Nature **394**, 453 (1998).
- [7] X. Chen et al., Phys. Rev. B **61**, 9782 (2000).
- [8] H. B. Jang et al., Sci Rep **10**, 3236 (2020).
- [9] L. Dreher et al., Phys. Rev. B **86**, 134415 (2012).
- [10] A. Kamra et al., Phys. Rev. B **91**, 104409 (2015).
- [11] Sergio C. Guerreiro and Sergio M. Rezende, Phys. Rev. B **92**, 214437 (2015).
- [12] C. Kittel, Phys. Rev. **110**, 836 (1958).
- [13] K. Uchida et al., Nat. Mater. **10**, 737 (2011).
- [14] K. Uchida, et al., Nat. Mater. **9**, 894 (2010).
- [15] S. Geprags et al., Appl. Phys. Lett. **96**, 142509 (2010).
- [16] M. Weiler et al., Phys. Rev. Lett. **108**, 176601 (2012).
- [17] E. I. Terukov et al., Phys. Status Solidi B **95**, 491 (1979).
- [18] Y. Fujii et al., Phys. Rev. B **11**, 2036 (1975).
- [19] R. Hühne et al., Supercond. Sci. Technol. **21**, 075020 (2008).
- [20] Kunihiko Irie et al., Jpn.J. Appl. Phys. **48**, 07GA01 (2009).
- [21] J. Bardeen, L. N. Cooper and J. R. Schrieffer, Phys. Rev. **108**, 1175 (1957).
- [22] J. Georg Bednorz and K. Alex Muller, Rev. Mod. Phys, **60**, 585 (1988).
- [23] K. Alex Muller, Z. Phys. B - Condensed Matter **80**, 193 (1990).
- [24] G.-H. Gweon et al. Nature **430**, 187 (2004).
- [25] J. Hwang et al., Nature **427**, 714 (2004).
- [26] Xiao-Jia Chen et al., Proc Natl Acad Sci USA, **104**, 3732 (2007).
- [27] Biswajit Dutta et al., Rev. Sci. Instrum. **91**, 123905 (2020).
- [28] G. W. Goodrich and J. x. lange, Phys.Rev **188**,728 (1969).
- [29] S B Roy et al., Supercond. Sci. Technol. **22**, 105014 (2009).
- [30] T F Smith, J. Phys. F: Met. Phys. **2**, 946 (1972).
- [31] Masanori Murakami and Tadashi Yogia, J. Appl. Phys. **57**, 211 (1985).
- [32] C. Clavero et al., Cryst. Growth Des. **12**, 2588 (2012).
- [33] Y. W. Kim et al., IEEE Transactions on Applied Superconductivity, **19**, 2649 (2009).
- [34] R. M. Moon and W. C. Kochler, Phys. Rev. B **4**, 1609 (1975).
- [35] B. Antic et al., Phys. Rev. B **58**, 3212 (1998).
- [36] Xiao-Jia Chen, Low Temp. Phys. **42**, 884 (2016).
- [37] Biswajit Dutta and A. Banerjee, Phys. Rev. B **106**, 134520 (2022).